NAS 1.60:1429

NASA Technical Paper 1429

COMPLETED
ORIGINAL

Exploratory Investigation of Two Resin-Matrix Composites Subjected to Arc-Tunnel Heating

Claud M. Pittman and Ronald D. Brown

MAY 1979

NASA

30

NASA Technical Paper 1429

Exploratory Investigation of Two Resin-Matrix Composites Subjected to Arc-Tunnel Heating

Claud M. Pittman and Ronald D. Brown
Langley Research Center
Hampton, Virginia

National Aeronautics
and Space Administration

**Scientific and Technical
Information Office**

1979

SUMMARY

Flexure and short-beam shear specimens of graphite-epoxy and graphite-polyimide composite material were subjected to seven arc-tunnel heating rates from 12.5 to 308 kW/m^2. The test-time duration varied from 5 to 1000 seconds. For each time and heating rate, the temperature response of the specimen was measured and the strength degradation was determined. Generally, as heating rates and test times increased, the strength degradation was greater with graphite-polyimide material less affected than graphite-epoxy material.

INTRODUCTION

The use of graphite-fiber/resin-matrix composite materials in the main structure of the Space Shuttle yields weight savings compared with conventional metallic materials. Graphite-epoxy composites are presently being used on the Space Shuttle payload-bay doors (ref. 1), and graphite-polyimide composites are being proposed for use in major parts of the Space Shuttle structure (ref. 2). In the event of a Shuttle heat-shield failure, the main structural skin of the vehicle will be subjected to aerodynamic heating (ref. 3). No information is presently available on the mechanical-property degradation of fiber-resin composite materials subjected to aerodynamic heating. However, because these composite materials should react to heating in much the same manner as a charring ablator, these composites may retain substantially more strength than would metal under similar conditions.

This paper describes the results of an exploratory investigation of the strength-retention characteristics of two composite materials subjected to simulated aerodynamic heating. Flexure and short-beam shear specimens of both a graphite-epoxy and a graphite-polyimide material were tested in an arc-tunnel environment. The materials were subjected to seven heating rates ranging from 12.5 to 308 kW/m^2 for test times from 5 to 1000 seconds. The range of heating rates selected includes those expected over most of the Shuttle surface area. The temperature response of the specimens was measured and the strength degradation caused by the various heating environments was determined.

Identification of commercial products in this report is to adequately describe the materials and does not constitute official endorsement, expressed or implied, of such products or manufacturers by the National Aeronautics and Space Administration.

ARC-TUNNEL TESTS

Test Specimens and Fixture

The graphite-epoxy material tested in this report was composed of A-S graphite fibers in 3501 epoxy resin[1] with a lay-up of $[0/+45/90/-45]_s$. The graphite-polyimide material was composed of HT-S graphite fiber[1] in NR150-B2 polyimide resin[2] with a lay-up of $[0/+45/-45/90]_s$. Graphite-epoxy flexure specimens were 16 ply and the graphite-polyimide flexure specimens were 8 ply. All short-beam shear specimens were 24 ply.

Each arc-tunnel test-specimen configuration consisted of a set of three flexure specimens and five short-beam shear specimens bonded to a fabric-reinforced phenolic support plate with a silicone-rubber adhesive (fig. 1). No primer was used with the adhesive so that the specimens could be removed more easily from the support plate after testing. The average dimensions of the test specimens are shown in figure 1. Note that the graphite-polyimide flexure specimens were only one-half the thickness of the graphite-epoxy flexure specimens. Two 30-gage chromel-alumel thermocouples were embedded in the bond line to measure the specimen back-surface temperature response.

The test specimen was mounted in a cast, fused-silica holder as shown in figure 2. A machine screw threaded into the backup plate held the plate in place. On the downstream side of the test specimen, a small spring-loaded fused-silica block was used in an attempt to accommodate thermal expansion in the flow direction. No practical solution for accommodating thermal expansion in the lateral direction was found.

The fused-silica specimen holder was mounted on the side of a water-cooled test fixture, as shown in figure 3. The surface of the block was about 0.60 cm below a rearward-facing step, because the heating-rate distribution over the surface of the specimen was more uniform with a rearward-facing step than with the specimen mounted flush with the fixture (ref. 4).

Test Environments

The arc tunnel used for the tests is described in reference 4. The test environments were selected to give a range of heating rates representative of the heating rates expected over most of the Shuttle surface area. The specific test environments used are given in table I.

The cold-wall heating rate was determined by the temperature-rise rate of a thin-skin calorimeter, as described in reference 5. The calorimeter configuration is shown in figure 4. The local pressure at the surface was measured with a calibration model of the same size and shape as the calorimeter. The heating-rate and pressure values given in table I were obtained at the center points of the respective models.

---

[1]A-S graphite fibers in 3501 epoxy resin, and HTR-S graphite fiber: products of Hercules Incorporated.

[2]NR150-B2 polyimide resin: product of E.I. du Pont de Nemours & Co., Inc.

Total enthalpy was determined by using probes to measure the stagnation heating rate and stagnation pressure in the center of the stream. A correlation equation was then used to calculate the enthalpy (ref. 6).

Test Procedure

The specimens were tested according to the matrix of heating rates and test times shown in table II. The arc-tunnel vacuum system limited the maximum test time to 1000 seconds. At heating rates greater than 21.6 kW/m^2, the behavior of the flexure specimens determined the maximum test time. Because of differential thermal expansion, some of the flexure specimens (especially the thinner graphite-polyimide specimens) partially debonded after some time in the test stream. When this debonding occurred, the test was terminated. Occasionally one of the three flexure specimens was lost down the tunnel before the test was stopped.

For each test, tunnel operating conditions were established and the test environment was allowed to stabilize. Heating-rate and pressure measurements were made and the specimen was inserted into the stream. After the specimen was removed from the stream, heating-rate and pressure measurements were repeated. Heating-rate and pressure measurements made before and after each test were essentially the same.

The output of the two thermocouples embedded in the bond line of each specimen was recorded during each test and until the temperatures peaked after the test. A pyrometer was used to measure the temperature of the heated surface during testing. When the edge of a flexure specimen debonded during the test, the edge that protruded into the stream became much hotter than the rest of the specimen. Also, when a surface ply was being removed, the surface temperature became much higher for a short time. For these reasons, great difficulty was encountered in obtaining a good measurement of the average surface temperature of the specimens.

MECHANICAL TESTS

The flexure specimens were tested according to reference 7, and the shear specimens were tested according to the short-beam method of reference 8. All specimens were tested with the heat-exposed side on two supports and the center load on the bond line side; thus, the heat-exposed side was in tension.

RESULTS AND DISCUSSION

Table II shows that the test times varied over a large range. For this reason, time is plotted on a logarithmic scale in the figures describing the test results.

Arc-Tunnel Tests

Graphite-epoxy tests.- The results of the arc-tunnel tests of the graphite-epoxy specimens are given in table III. The average maximum back-surface temperature rise for each test is shown in figure 5. As expected, longer test times and higher heating rates resulted in greater back-surface temperature rises.

The data for back-surface temperature rise are plotted as a function of total cold-wall heat input to the surface in figure 6. As expected, the temperature rise is, in general, larger with larger total heat inputs. Figure 6 is presented primarily to provide a measure of the scatter in these data.

The data for approximate maximum front-surface temperature are plotted in figure 7. The radiation-equilibrium temperature for each heating rate is also shown. An emittance of 1 was assumed for all temperatures. At the lowest heating rate, the specimens attained a steady-state temperature condition by 500 seconds. The temperature rise with time was monotonically larger with heating rate. The large differences between the surface temperature and the radiation-equilibrium temperature indicate that conduction was an important heat-accommodation mechanism with the model configuration used.

Graphite-polyimide tests.- The results of the arc-tunnel tests of the graphite-polyimide specimens are given in table IV. The average maximum back-surface temperature rise for each test is shown in figure 8. The data were not consistent, especially the variation in temperature rise with time at a particular heating rate. The primary problem encountered was that during testing, an end or an edge of one or two of the flexure specimens pulled away from the bond line. This partial failure probably occurred much more frequently in these tests because the graphite-polyimide specimens were much thinner than the graphite-epoxy specimens; therefore, thermal expansion effects were more severe.

The average maximum back-surface temperature rise is plotted as a function of total cold-wall heat input to the surface in figure 9. Although the trend of the data is similar to the trend in figure 6, the scatter is much greater.

The data for approximate maximum front-surface temperature and the radiation-equilibrium temperatures are shown in figure 10. The values and trends are similar to those shown in figure 7. At all heating rates except the two lowest, the front-surface temperature rise for longer test times was less for the graphite-polyimide material than for the graphite-epoxy material. These results may indicate different surface-emittance changes in the two materials as surface degradation occurred.

Mechanical Property Tests

Graphite-epoxy tests.- The results of the graphite-epoxy mechanical-property tests are given in table III. The ratio of exposed- to unexposed-specimen strengths for flexure and short-beam shear specimens is given. The

average-strength ratios for the specimens in each arc-tunnel test are given. The unexposed-specimen dimensions were used to calculate the exposed-specimen strengths.

The flexure strength-retention ratios for each heating rate are plotted in figure 11 as a function of exposure time. At the lowest heating rate, the strength of the material was not affected, even for the longest exposure time. At all other heating rates, the strength was significantly lower for the longer test times.

The specimens were examined after the tests to determine the failure modes. Nearly all the flexure specimens with strength ratios more than 0.5 failed in tension on the heated side. Most of the specimens with strength ratios less than 0.5 failed in shear, usually near the heated surface.

Typical photomicrographs of flexure-specimen cross sections are shown in figure 12. The heated side of each specimen is at the top. Figure 12(a) shows specimen 2, which was tested at 12.5 kW/m^2 for 1000 seconds. The epoxy in the outer 0° ply was 50 to 75 percent charred. This specimen showed no strength degradation and failed in tension. Specimen 4, which was tested at 21.6 kW/m^2 for 600 seconds and had a strength-retention ratio of 0.10, is shown in figure 12(b). This specimen was typical of the specimens which showed severe strength degradation. The outer 0° ply was gone, the epoxy in the $+45^\circ$ and 90° plies was charred, and the epoxy was partially charred in the -45° and the second 0° plies. This specimen failed in shear.

Figure 12(c) shows specimen 13, which was tested at 70 kW/m^2 for 50 seconds and had a strength-retention ratio of 0.42. The outer 0° ply was gone, the epoxy in the $+45^\circ$ ply was charred, and the 90° ply was partially charred. This specimen also failed in shear. Figure 12(d) shows specimen 17, which was tested at 308 kW/m^2 for 9 seconds and had a strength-retention ratio of 0.64. The outer 0° ply was gone, the epoxy in the $+45^\circ$ ply was charred, and the 90° and -45° plies were partially charred. This specimen failed in tension.

Specimens 4, 13, and 17 are not greatly different in visible degradation, although the strength-retention ratios were 0.10, 0.42, and 0.64, respectively. The respective test times were 600, 50, and 9 seconds. These results indicate a time-dependent degradation effect that reduces material strength but is not visible in the photomicrographs.

The computer program described in reference 9 was used to explore the feasibility of developing a capability for predicting flexure strength retention from the condition of the exposed specimens. The stiffness matrix for the 16-ply specimen was calculated and the failure load for the unexposed specimens was used to obtain a failure strain, which was 1.2 percent. Stiffness matrices were then calculated for 12 plies (down to the next 0° ply) and 5 plies (down to the third 0° ply). These stiffness matrices were used with the 1.2-percent failure strain to calculate failure loads for the reduced thicknesses. These two failure loads gave strength ratios of 0.59 and 0.15.

The analytical results are only applicable to a tension failure in the 0° ply; therefore, specimens 4 and 13 (figs. 12(b) and 12(c)), which failed in

shear, are not represented by the analysis. Specimen 2 (fig. 12(a)) failed in tension with no strength degradation, even though the outer ply was partially charred. This result indicates that epoxy charred at a low temperature retains sufficient integrity to transfer load within the ply. Specimen 17 (fig. 12(d)), which failed in tension with the outer 0° ply missing, had a strength-retention ratio of 0.64. This agrees well with the analytically predicted strength retention of 59 percent (12 plies). This failure indicates that the outer $+45^{\circ}$, 90°, and -45° plies, as expected, did not contribute significantly to the tensile strength.

The short-beam shear test data are shown in figure 13. The data trends are very similar to those of the flexure data in figure 11 except for the results at a heating rate of 161 kW/m^2. No reason was found for the inconsistency of the data at this heating rate. All short-beam shear specimens failed in shear. For specimens with low strength ratios, the shear cracks were nearer the heated side.

Figures 11 and 13 were used to obtain a plot of heating rate versus time for an arbitrarily selected strength-retention ratio of 0.75. The result is shown in figure 14. The figure shows good agreement between the flexure and short-beam shear data. Although the failure mechanisms were, in general, different for the two types of specimens, matrix degradation appeared to affect the strength retention of both types of specimens to about the same extent.

Graphite-polyimide tests.- The results of the graphite-polyimide mechanical tests are given in table IV as ratios of exposed- to unexposed-specimen strengths. Examination of the exposed flexure specimens showed mostly tension failures at the heated surface. A few of the most severely degraded specimens failed in shear, with the shear cracks tending to be nearer the heated surface. The short-beam shear specimens failed in shear, with the shear cracks near the center of all specimens.

Typical photomicrographs of flexure-specimen cross sections are shown in figure 15. The heated side of each specimen is at the top. Figure 15(a) shows specimen 22, which was tested at 21.6 kW/m^2 for 600 seconds and had a strength-retention ratio of 0.84. The outer 0° ply was slightly charred. Figure 15(b) shows specimen 28, which was tested at 59 kW/m^2 for 100 seconds and had a strength-retention ratio of 0.76. The outer 0° ply was about 30 percent charred.

Figure 15(c) shows specimen 31, which was tested at 70 kW/m^2 for 40 seconds and had a strength-retention ratio of 0.55. The outer 0° ply was about 50 percent charred. Figure 15(d) shows specimen 33, which was tested at 161 kW/m^2 for 18 seconds and had a strength-retention ratio of 0.23. The outer 0° ply was over 50 percent charred and the interfaces between the 0° and $+45^{\circ}$ plies and between the $+45^{\circ}$ and -45° plies were charred. None of the specimens lost the outer 0° ply, indicating that the polyimide developed into a very tough char.

The flexure strength-retention ratios are plotted in figure 16. At the lowest heating rate, the strength of the material was not affected, even for the longest exposure time. The data trends are then consistent, with the strength-retention ratio being lower for higher heating rates and longer times. The strength-retention ratios at the two highest heating rates are lower than

those for the corresponding graphite-epoxy specimens. However, the graphite-epoxy specimens were twice as thick as the graphite-polyimide specimens, and considerably more undegraded graphite-epoxy remained after testing. Therefore, although the polyimide provides a more thermally stable matrix material, the lower strength-retention ratios which were obtained are reasonable. This argument is reinforced by the short-beam shear data for graphite-polyimide specimens given in table IV. Only for the 11-second test at the highest heating rate was any significant strength degradation measured. The short-beam shear specimens were all the same thickness, so the more thermally stable polyimide matrix degraded much less than the epoxy at the same test conditions.

CONCLUDING REMARKS

Flexure and short-beam shear specimens of a graphite-epoxy and a graphite-polyimide material were tested in an arc-tunnel environment at several heating rates and test times. The temperature response of the specimens was measured and the strength degradation caused by the various heating environments was determined.

The flexure and short-beam shear strengths of both materials were essentially unaffected at the lowest heating rate (12.5 kW/m^2). At the other heating rates, the graphite-epoxy test data were consistent, showing more degradation at higher heating rates and longer test times. The test data for the graphite-polyimide flexure specimens were inconsistent because the specimens were too thin to give good test results with the test configuration used. The good thermal stability of the polyimide matrix material was shown by the short-beam shear test data, which showed strength degradation only at the most severe test condition.

Good agreement was obtained between the graphite-epoxy flexure and short-beam shear data when the test time for an arbitrarily selected strength-retention ratio of 0.75 was plotted as a function of heating rate. Although the failure mechanisms were, in general, different for the two types of specimens, matrix degradation appeared to affect the strength retention of both types of specimens to about the same extent.

Langley Research Center
National Aeronautics and Space Administration
Hampton, VA 23665
March 29, 1979

REFERENCES

1. Bruner, R. C.: Materials Selection for the Space Shuttle Orbiter Payload Bay Doors. Bicentennial of Materials Progress, Volume 21 of National SAMPE Symposium and Exhibition, Soc. Advance. Mater. & Process Eng., 1976, pp. 459-473.

2. Davis, John G., Jr.: Composites for Advanced Space Transportation Systems - CASTS. NASA TM-80038, 1978.

3. Hunt, L. Roane: Aerodynamic Heating in Large Cavities in an Array of RSI Tiles. NASA TN D-8400, 1977.

4. Brown, Ronald D.; and Jakubowski, Antoni K.: Heat-Transfer and Pressure Distributions for Laminar Separated Flows Downstream of Rearward-Facing Steps With and Without Mass Suction. NASA TN D-7430, 1974.

5. Standard Method for Design and Use of a Thin-Skin Calorimeter for Measuring Heat Transfer Rate. ASTM Designation: E 459 - 72. Part 41 of 1977 Annual Book of ASTM Standards, c.1977, pp. 601-607.

6. Pittman, Claud M.; and Brown, Ronald D.: Surface Recession Characteristics of a Cryogenic Insulation Subjected to Arc-Tunnel Heating. NASA TM X-3291, 1975.

7. Standard Test Methods for Flexural Properties of Plastics and Electrical Insulating Materials. ANSI/ASTM D 790 - 71. Part 35 of 1977 Book of ASTM Standards, 1977, pp. 308-317.

8. Standard Test Method for Apparent Horizontal Shear Strength of Reinforced Plastics by Short Beam Method. ANSI/ASTM D 2344 - 76. Part 36 of 1977 Book of ASTM Standards, 1977, pp. 351-354.

9. Muha, T. J.: Users' Manual for the Laminate Point Stress Analysis Computer Program SQ5 as Revised by AFFDL/FBC. AFFDL-TM 74-107-FBC, U.S. Air Force, July 1974.

TABLE I.- TEST ENVIRONMENTS

Heating rate, kW/m^2	Enthalpy, MJ/kg	Local pressure at surface, atm[a]	Wedge angle of attack, deg
12.5	1.39	0.0057	3
21.6	2.92	.0029	3
31.8	3.36	.0047	3
59	7.22	.0032	3
70	7.84	.0038	3
161	6.22	.033	30
308	8.26	.066	30

[a]1 atm = 101.3 kPa.

TABLE II.- MATRIX OF HEATING RATES AND TEST TIMES

Heating rate, kW/m^2	Test time, s	
	Graphite-epoxy	Graphite-polyimide
12.5	500, 1000	500, 1000
21.6	200, 600, 1000	200, 400, 600
31.8	50, 100, 300	50, 88, 176
59	50, 100, 145	50, 80, 100
70	20, 50	20, 30, 40
161	10, 16	10, 18
308	5, 9	5, 11

TABLE III.- GRAPHITE-EPOXY TEST RESULTS

Specimen	Heating rate, kW/m^2	Test time, s	Back-surface temperature rise, K	Front surface temperature, K	Strength-retention ratio	
					Flexure	Short-beam shear
1	12.5	500	163	481	1.00	1.00
2	12.5	1000	189	481	1.00	1.00
3	21.6	200	176	556	1.00	1.00
4	21.6	600	214	667	.10	.16
5	21.6	1000	242	706	.04	.07
6	31.8	50	101	589	1.00	1.00
7	31.8	100	159	667	.95	1.00
8	31.8	300	206	836	.06	.33
9	59	50	113	600	.94	1.00
10	59	100	179	833	.27	.59
11	59	145	198	922	.03	.20
12	70	20	79	589	1.00	1.00
13	70	50	154	922	.42	.68
14	161	10	108	850	.93	.82
15	161	16	132	1067	.62	.87
16	308	5	97	1006	.78	.85
17	308	9	109	1256	.64	.26

TABLE IV.- GRAPHITE-POLYIMIDE TEST RESULTS

Specimen	Heating rate, kW/m^2	Test time, s	Back-surface temperature rise, K	Front-surface temperature, K	Strength-retention ratio	
					Flexure	Short-beam shear
18	12.5	500	168	478	1.00	1.00
19	12.5	1000	186	478	1.00	1.00
20	21.6	200	187	583	1.00	1.00
21	21.6	400	251	669	.88	1.00
22	21.6	600	245	767	.84	1.00
23	31.8	50	123	600	1.00	1.00
24	31.8	88	163	644	1.00	1.00
25	31.8	176	164	694	.92	1.00
26	59	50	166	722	.83	1.00
27	59	80	227	778	.78	1.00
28	59	100	202	811	.76	1.00
29	70	20	106	672	1.00	1.00
30	70	30	87	767	.67	1.00
31	70	40	185	811	.55	1.00
32	161	10	162	917	.58	1.00
33	161	18	168	1122	.23	1.00
34	308	5	97	1047	.33	1.00
35	308	11	144	1167	.04	.70

Specimen and material type	Thickness, cm	Width, cm	Length, cm
Flexure:			
Graphite-epoxy	0.22	1.18	7.62
Graphite-polyimide	0.11	1.27	7.62
Short-beam shear:			
Graphite-epoxy	0.32	0.66	1.60
Graphite-polyimide	0.32	0.66	1.59

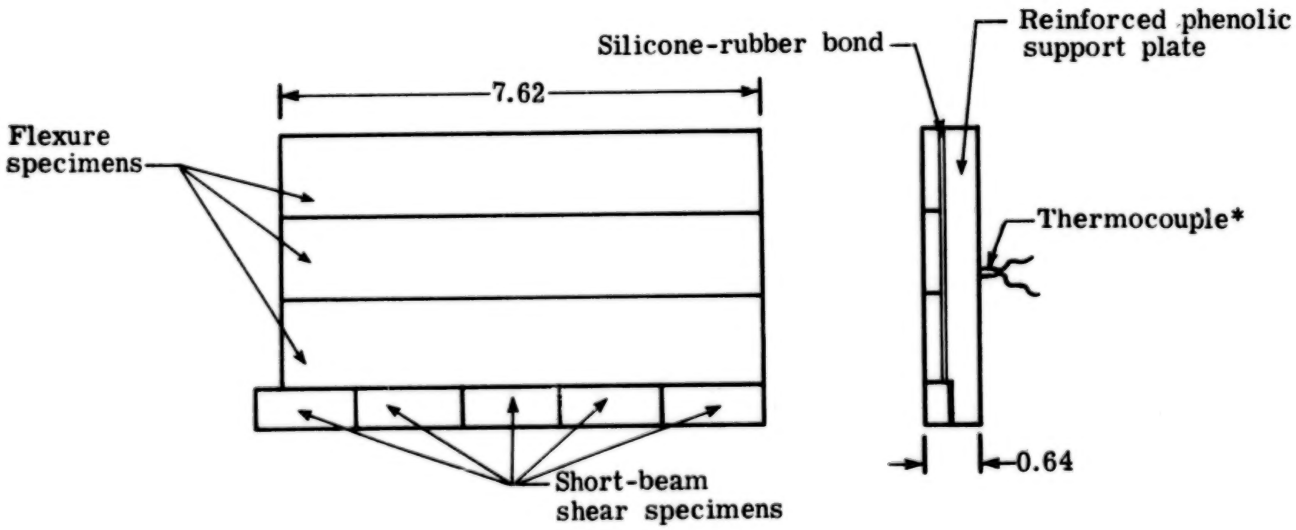

*Two no. 30-gage thermocouples were embedded in the bond-line, 1.78 cm from each edge.

Figure 1.- Test-specimen configuration. Dimensions are in cm.

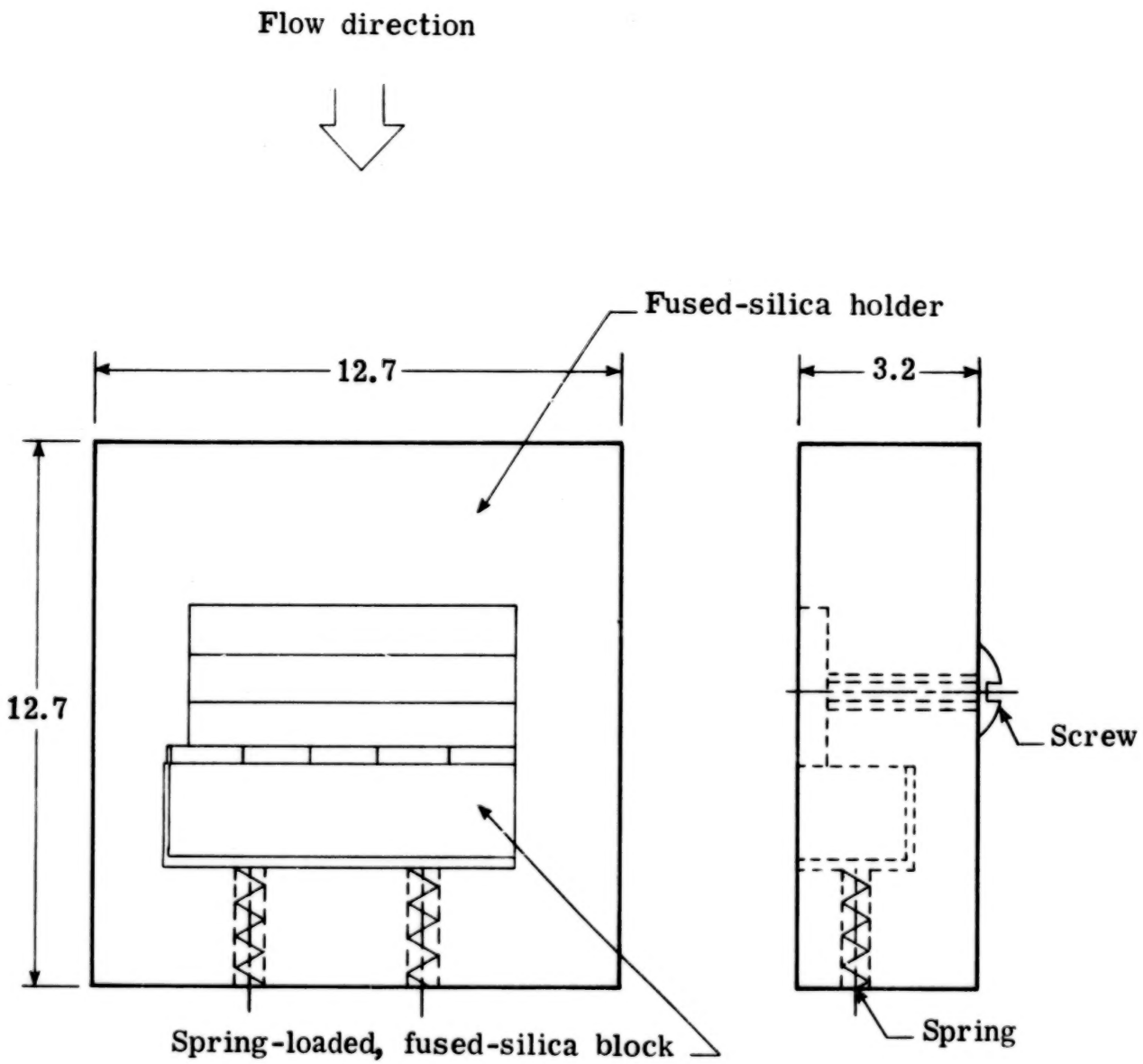

Figure 2.- Fused-silica holder with test specimen. Dimensions are in cm.

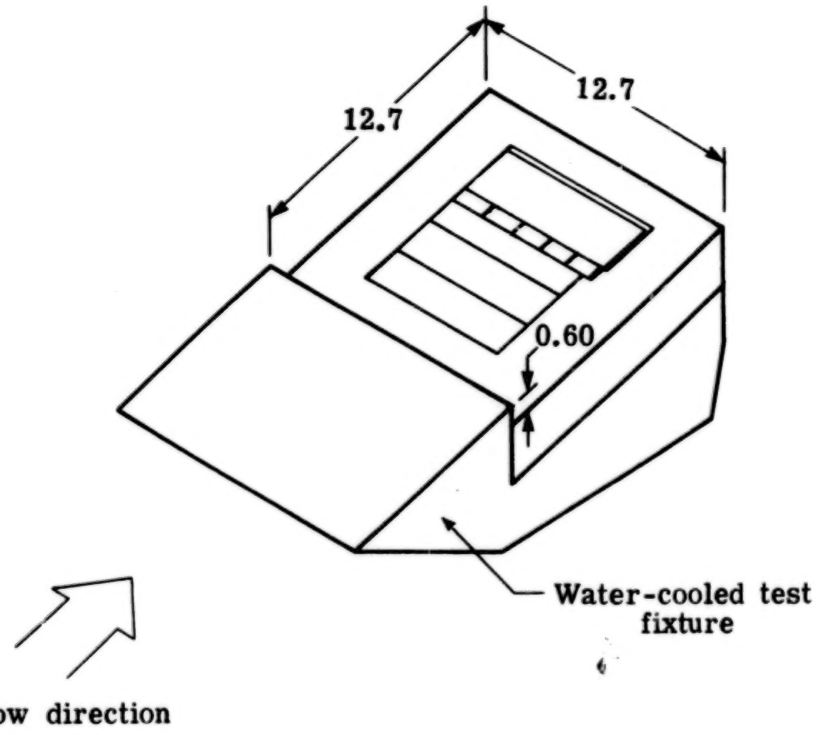

Figure 3.- Arc-tunnel test specimen configuration. Dimensions are in cm.

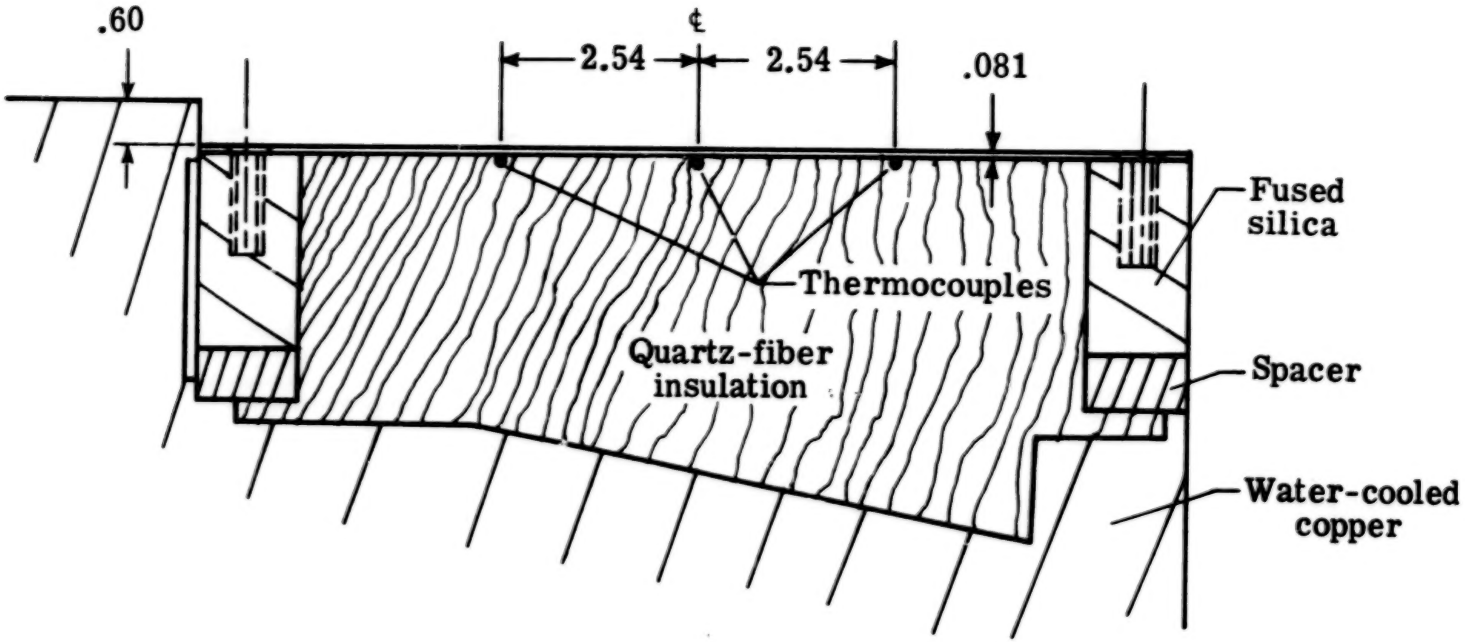

Figure 4.- Arc-tunnel calorimeter configuration. Dimensions are in cm.

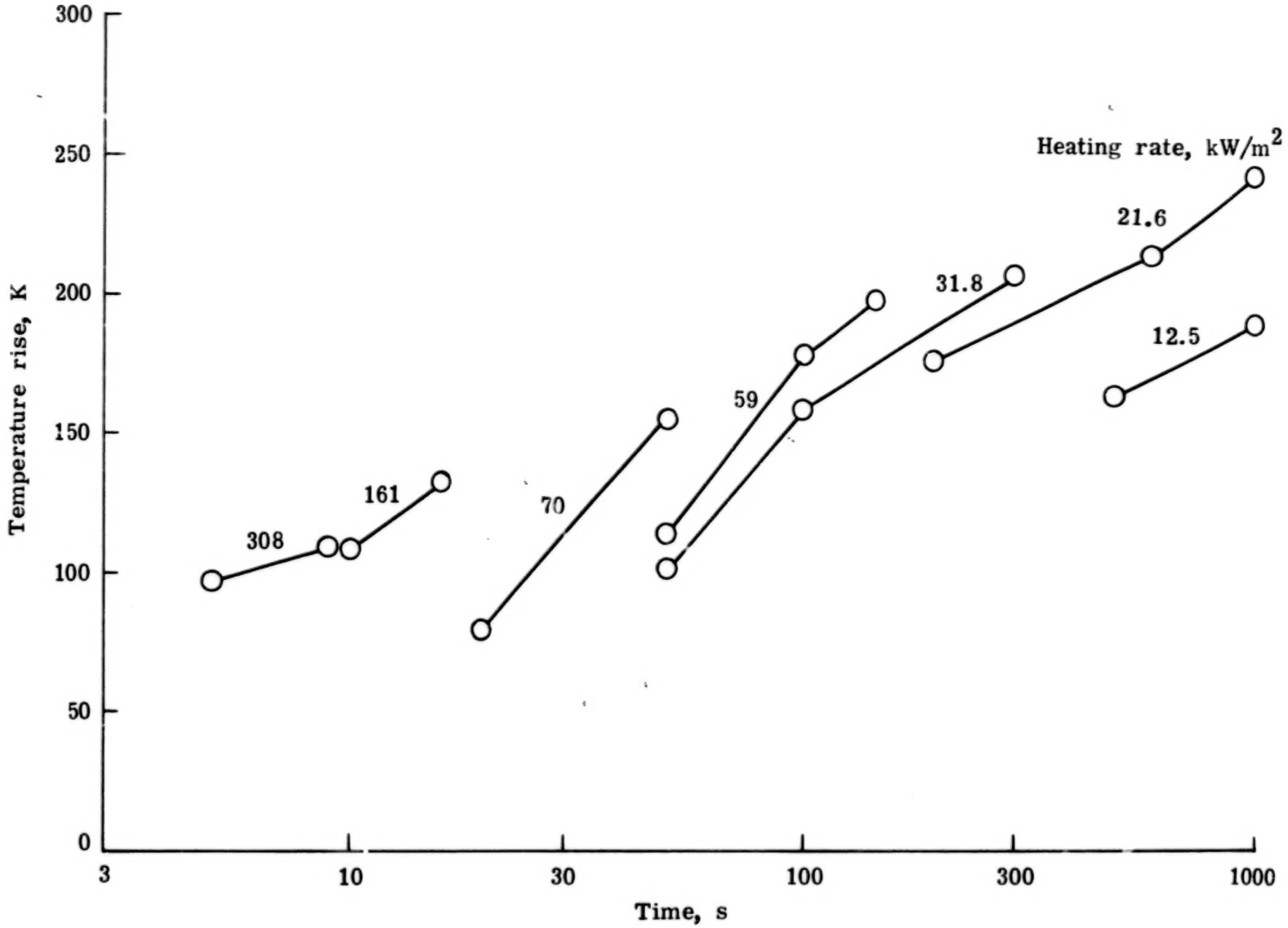

Figure 5.- Back-surface temperature rise for graphite-epoxy specimens.

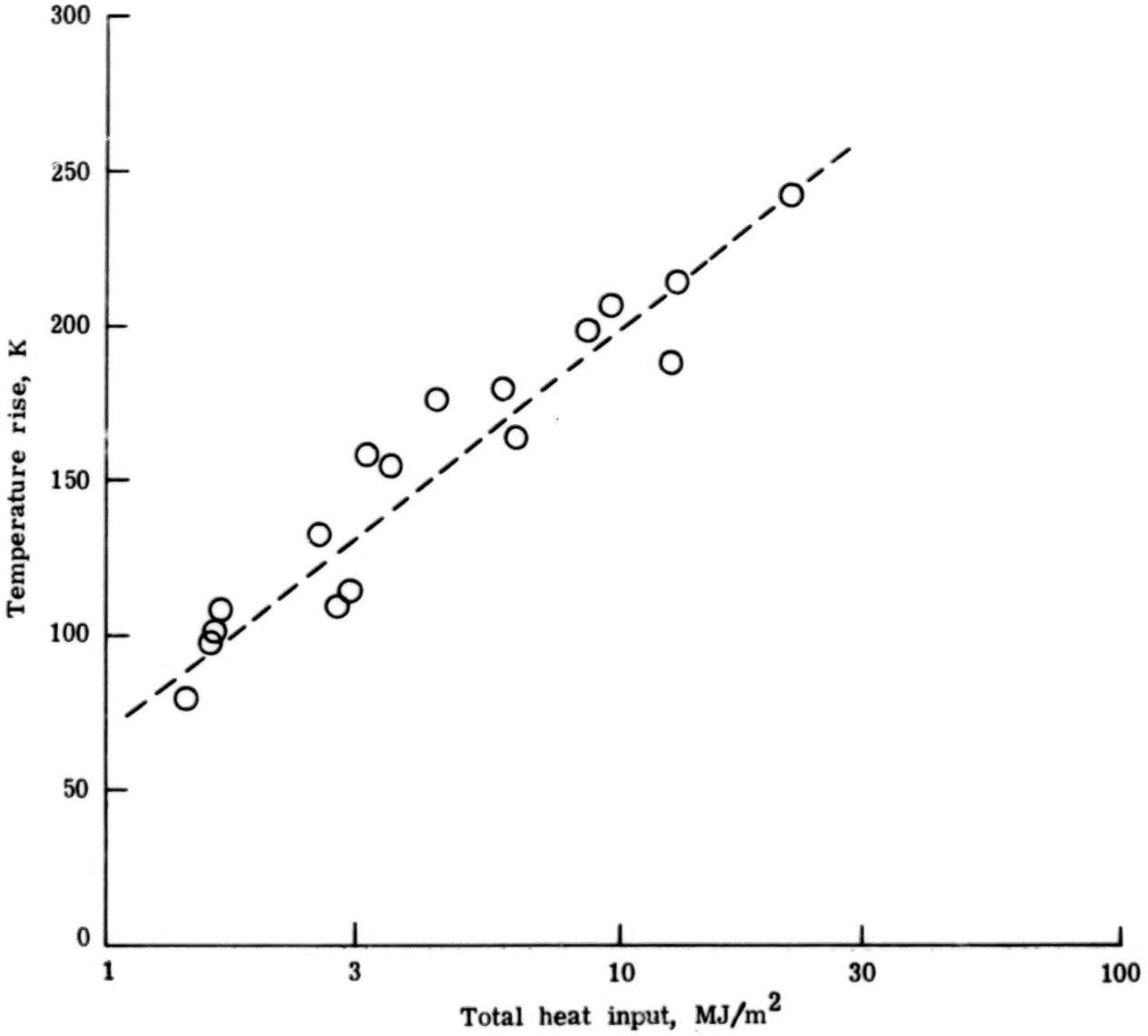

Figure 6.- Back-surface temperature rise vs total heat input for graphite-epoxy specimens.

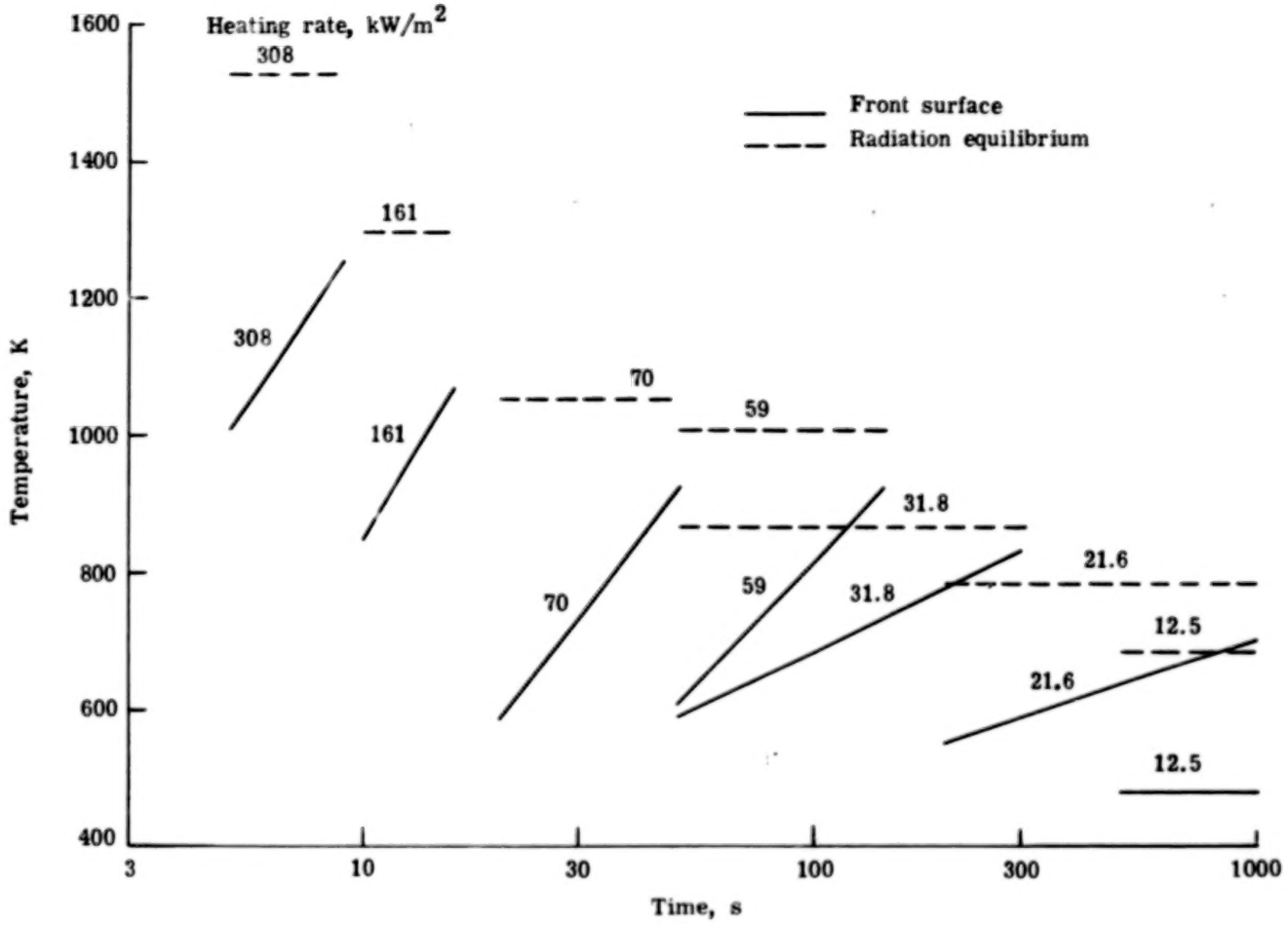

Figure 7.- Approximate front-surface temperatures and radiation-equilibrium temperatures for graphite-epoxy specimens. Emittance, 1.0.

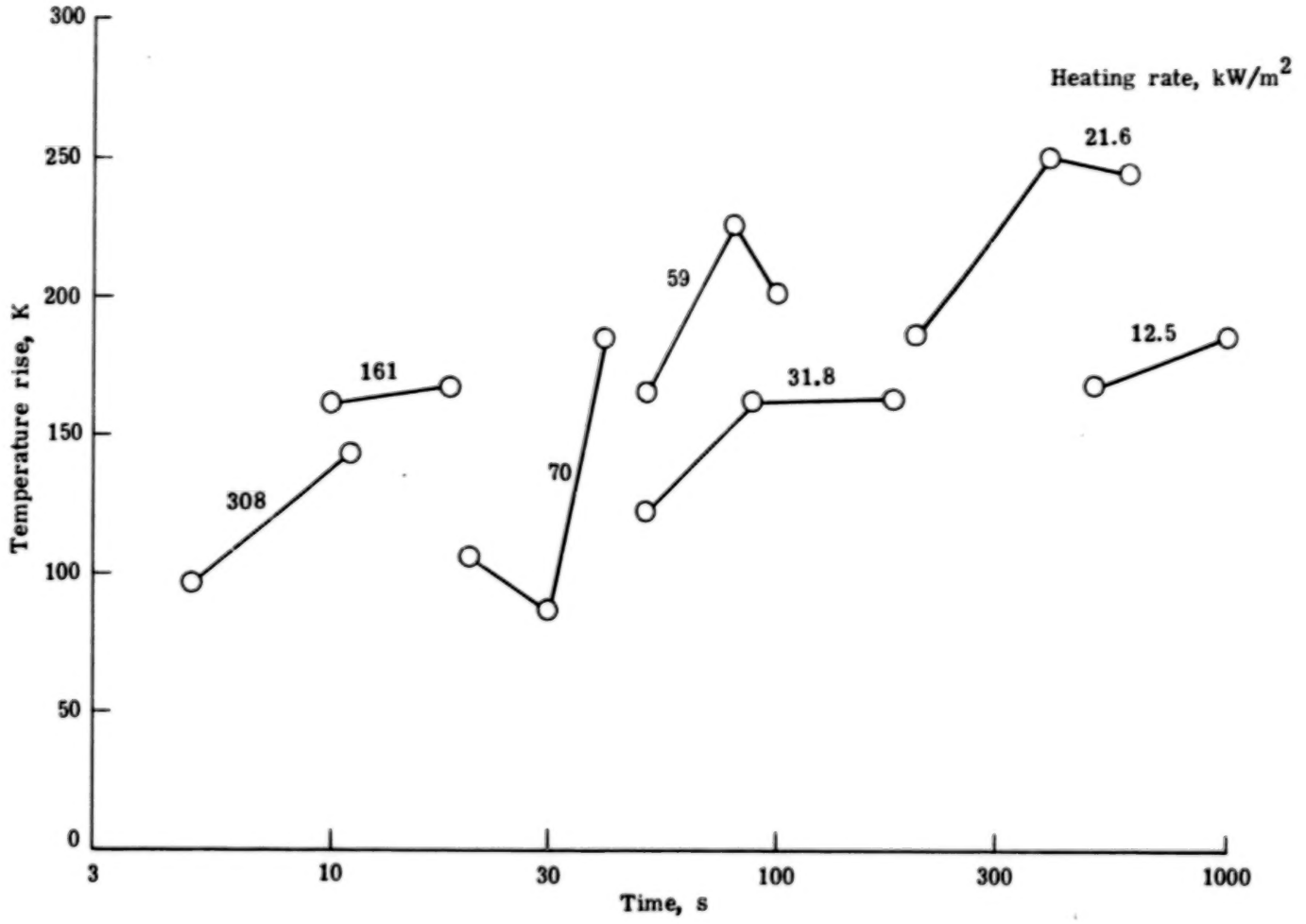

Figure 8.- Back-surface temperature rise for graphite-polyimide specimens.

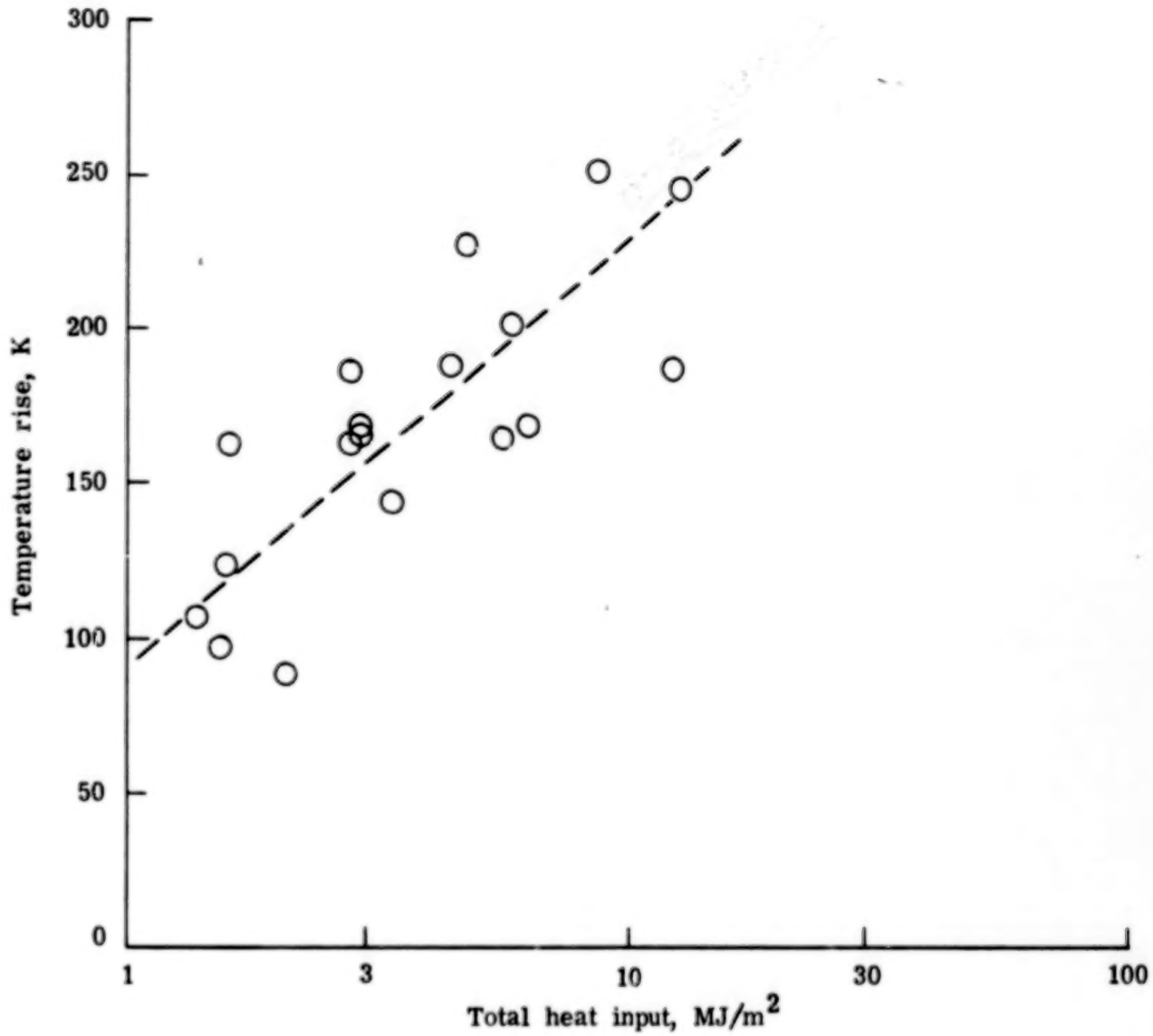

Figure 9.- Back-surface temperature rise vs total heat input for graphite-polyimide specimens.

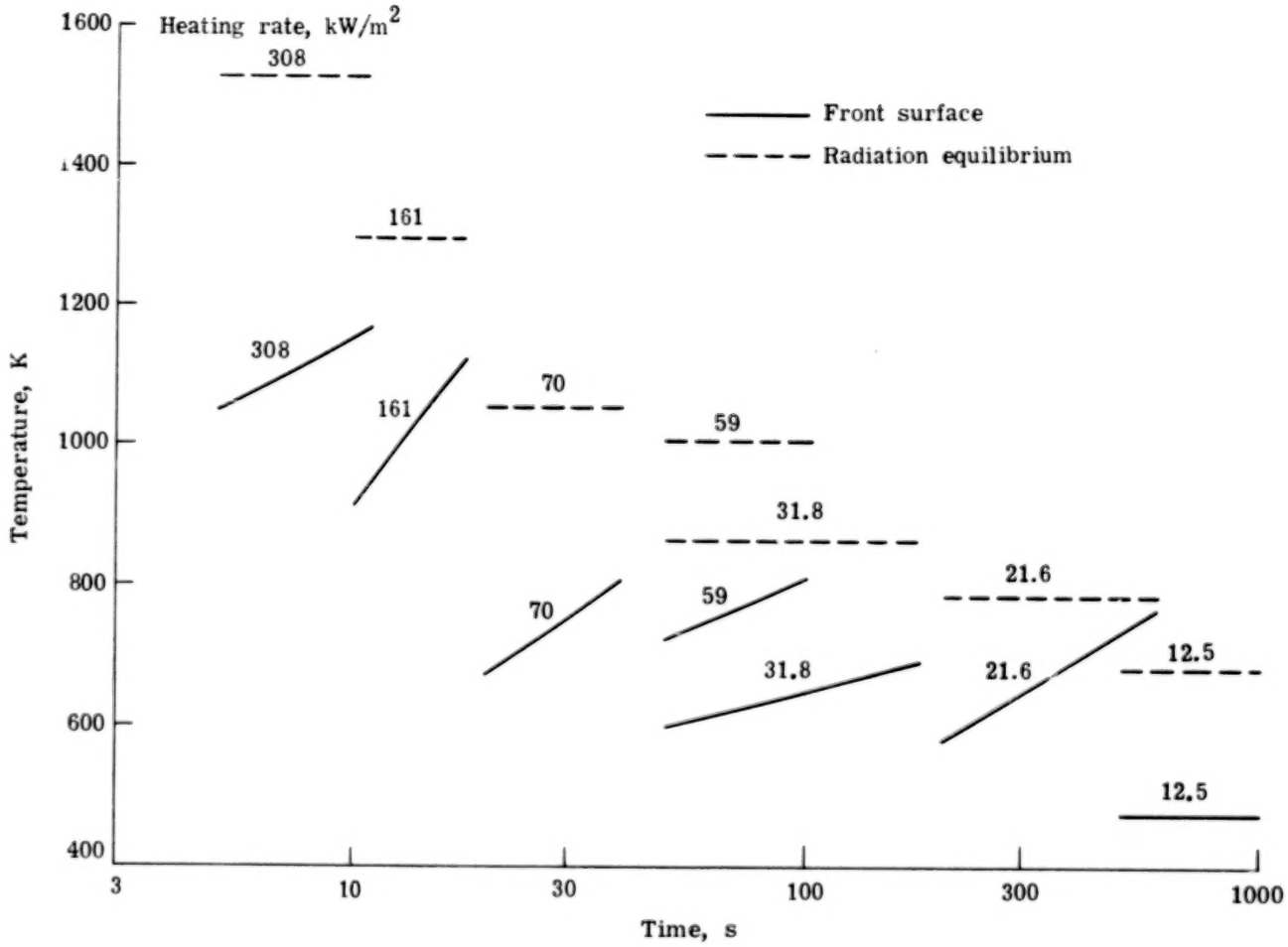

Figure 10.- Approximate front-surface temperatures and radiation-equilibrium temperatures for graphite-polyimide specimens. Emittance, 1.0.

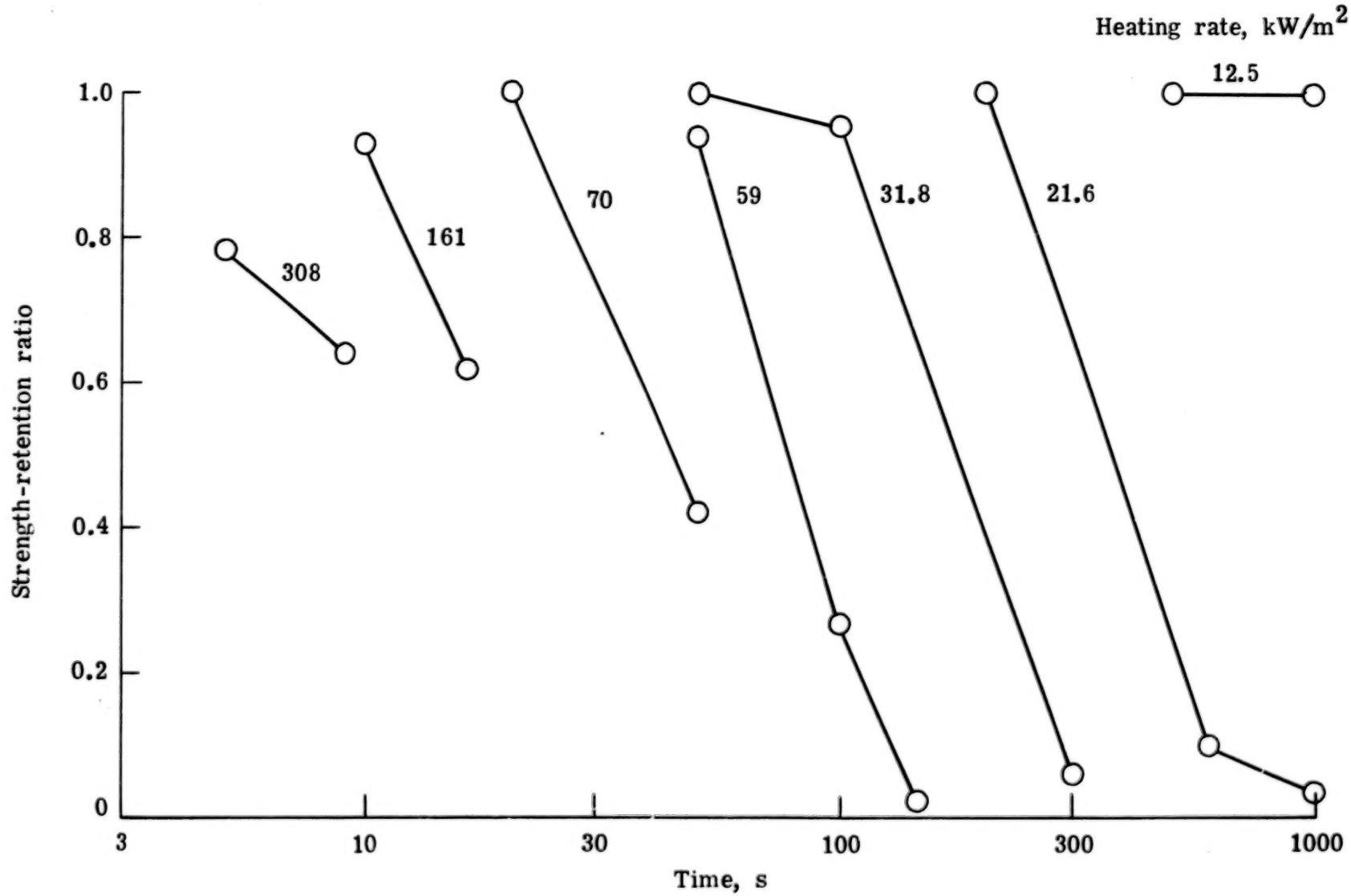

Figure 11.- Flexure strength-retention ratios of graphite-epoxy specimens.

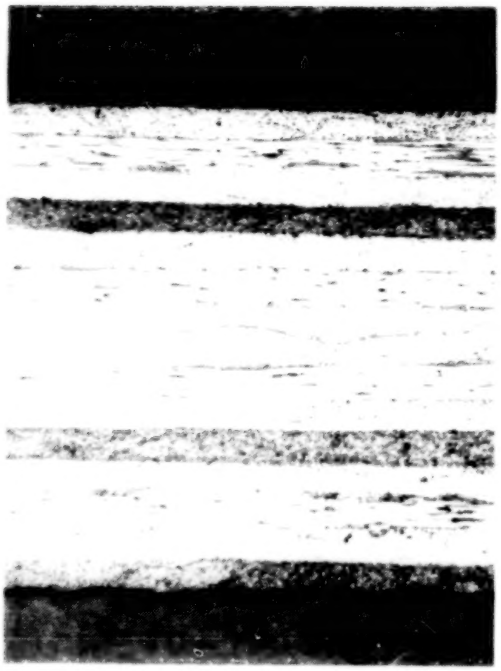

(a) Specimen 2 (heating rate, 12.5 kW/m^2; test time, 1000 s).

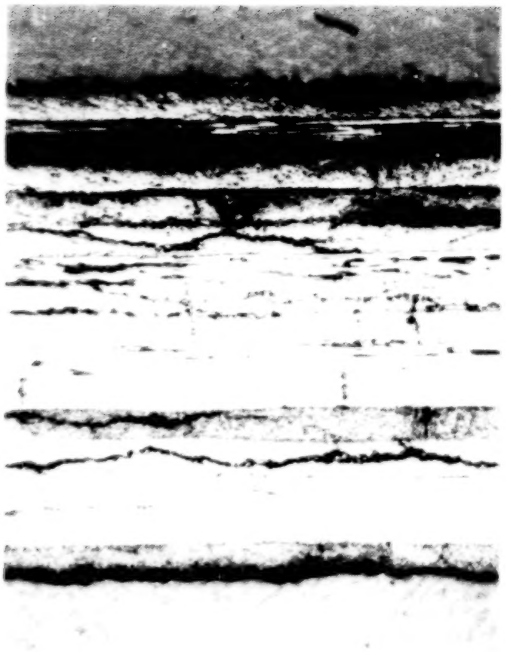

(b) Specimen 4 (heating rate, 21.6 kW/m^2; test time, 600 s).

(c) Specimen 13 (heating rate, 70 kW/m^2; test time, 50 s).

(d) Specimen 17 (heating rate, 308 kW/m^2; test time, 9 s).

L-79-138

Figure 12.- Photomicrographs of typical graphite-epoxy flexure specimen cross sections (×31).

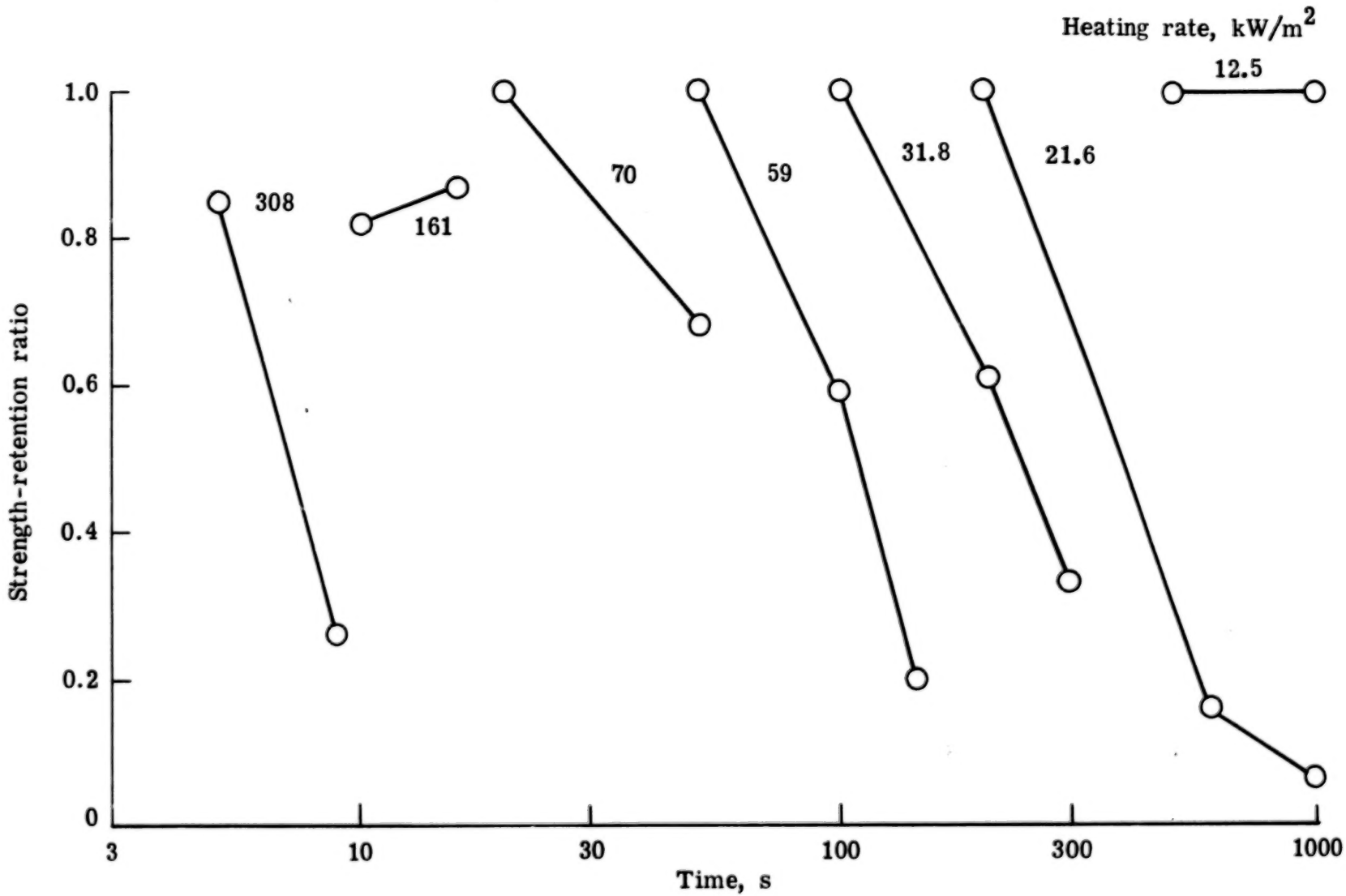

Figure 13.- Short-beam shear strength-retention ratios for graphite-epoxy specimens.

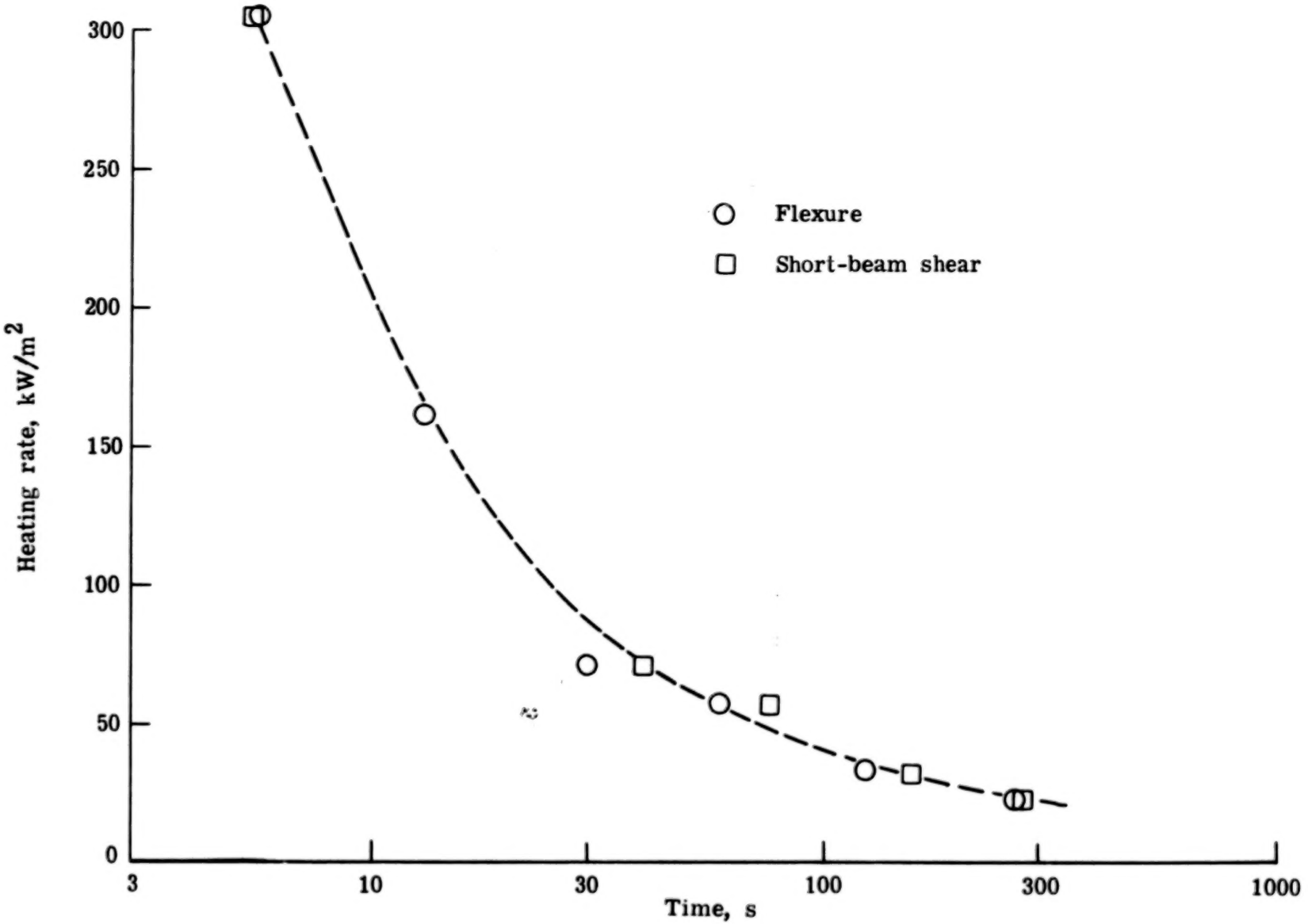

Figure 14.- Heating rate vs time for a strength-retention ratio of 0.75 of graphite-epoxy specimens.

(a) Specimen 22 (heating rate, 21.6 kW/m^2; test time, 600 s).

(b) Specimen 28 (heating rate, 59 kW/m^2; test time, 100 s).

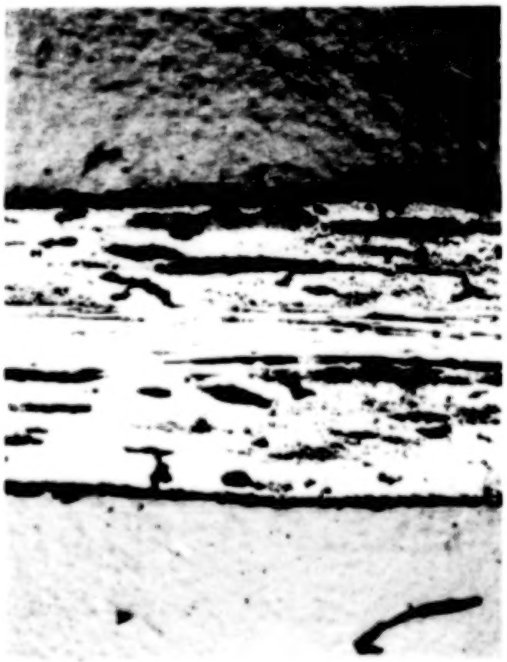

(c) Specimen 31 (heating rate, 70 kW/m^2; test time, 40 s).

(d) Specimen 33 (heating rate, 161 kW/m^2; test time, 18 s).

L-79-139

Figure 15.- Photomicrographs of typical graphite-polyimide flexure specimen cross sections (×31).

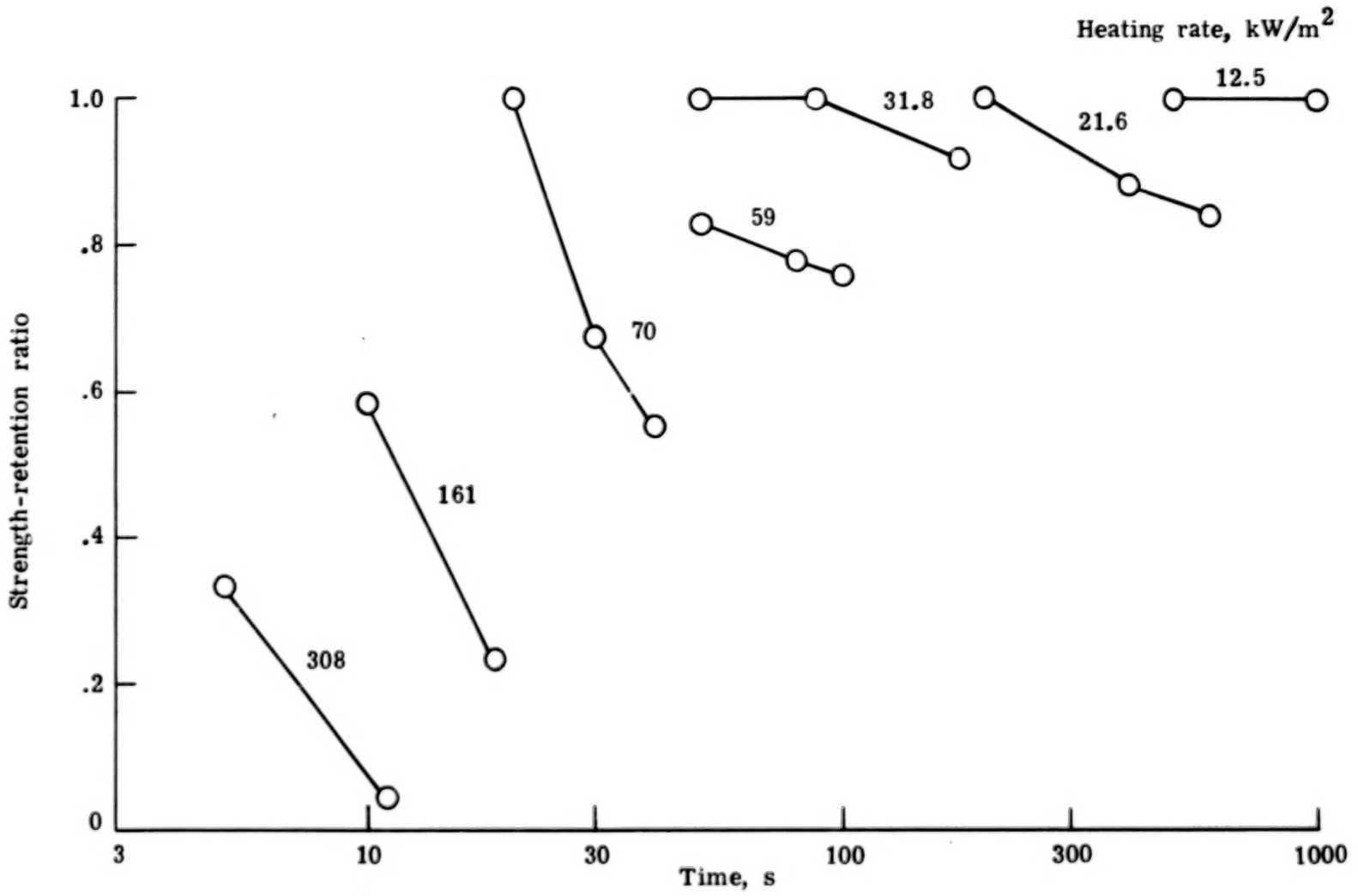

Figure 16.- Flexure strength-retention ratios of graphite-polyimide specimens.

1. Report No.	2. Government Accession No.	3. Recipient's Catalog No.
NASA TP-1429		

4. Title and Subtitle	5. Report Date
EXPLORATORY INVESTIGATION OF TWO RESIN-MATRIX COMPOSITES SUBJECTED TO ARC-TUNNEL HEATING	May 1979
	6. Performing Organization Code
7. Author(s)	8. Performing Organization Report No.
Claud M. Pittman and Ronald D. Brown	L-12665
	10. Work Unit No. 524-71-03-04
9. Performing Organization Name and Address	11. Contract or Grant No.
NASA Langley Research Center Hampton, VA 23665	
	13. Type of Report and Period Covered
12. Sponsoring Agency Name and Address	Technical Paper
National Aeronautics and Space Administration Washington, DC 20546	14. Sponsoring Agency Code

15. Supplementary Notes

16. Abstract

Flexure and short-beam shear specimens of a graphite-epoxy and a graphite-polyimide composite material were tested in an arc-tunnel environment. The materials were subjected to seven heating rates from 12.5 to 308 kW/m^2 for test times from 5 to 1000 seconds. The temperature response of the specimens was measured and the strength degradation caused by the various heating environments was determined.

17. Key Words (Suggested by Author(s))

Composite materials
Aerodynamic heating
Mechanical tests

18. Distribution Statement

Unclassified - Unlimited

Subject Category 24

19. Security Classif. (of this report)	20. Security Classif. (of this page)	21. No. of Pages	22. Price*
Unclassified	Unclassified	27	$4.50

* For sale by the National Technical Information Service, Springfield, Virginia 22161

NASA-Langley, 1979

END

September 11, 1979